# ANALYSIS AND OPTIMIZATION OF JOINT FORMATION IN HYBRID COMPRESSION MOLDING

J. Lückenkötter[1*], S. Aydin[1], T. Marten[1] and T. Tröster[1]

[1] Chair for Automotive Lightweight Design, University of Paderborn, Paderborn, Germany
*Julian Lückenkötter (julian.lueckenkoetter@upb.de)

**Keywords:** compression molding, in-mold-assembly, hybrid components, joint characterization

## ABSTRACT

Outstanding weight-specific properties of fiber-reinforced plastics (FRP) make it possible to contribute significantly to the minimization of greenhouse gases by reducing moving masses through substitution of existing metal structures. Whereas thermoset-based FRP are only used in high-end applications such as motor sports or in the aerospace sector due to high material costs and a complex manufacturing process, fiber-reinforced thermoplastics offer an opportunity for economical lightweight construction. A partial combination of FRP with metals can maximize the weight-specific properties of a component and compensate the material-specific disadvantages. Components based on glass fiber mat-reinforced thermoplastics produced by compression molding are particularly promising in this context, as they have an advantageous property profile in addition to a high degree of design freedom. To maximize efficiency, the molding of the FRP and the bonding to the metal should take place in a single process step (in-mold assembly). Due to a low affinity of polypropylene (PP)-based FRP to metallic materials, an adhesion promoter is always necessary for hybridization. In the present study, the joint formation in a one-shot process will be analyzed based on the main process parameters. In addition, it will be verified that the generated joint is suitable for relevant load cases.

## 1 INTRODUCTION

In the development of cars, the reduction of resource and energy consumption as well as carbon dioxide emissions represent important objectives. Innovative lightweight design strategies can make a significant contribution in this context by minimizing mass-dependent driving resistances and thus energy consumption during driving. This approach can also be applied to all other transportation sectors (commercial vehicles, aircraft, etc.), making lightweight design a widespread goal [1].

Due to their outstanding weight-specific mechanical properties, fiber-reinforced plastic composites offer high potential for lightweight construction. In terms of process times, material costs and recyclability at the end of a life cycle, FRP with thermoplastic matrix (tFRP) take a leading role in contrast to thermoset FRP [2-4]. The application of glass mat-reinforced thermoplastics (GMT) in the compression molding process is particularly promising. GMT has much higher mechanical properties than plastic granulate processed by injection molding due to greater fiber length of up to 50 mm. In addition, a nearly isotropic mechanical property profile and a high degree of design freedom are present [2].

In contrast, metals are usually used to achieve high mechanical performance (e.g. high tensile strengths or stiffnesses) or certain physical properties (e.g. thermal and electrical conductivity). Lightweight design approaches for metallic materials are based on reducing wall thicknesses while using high-strength alloys. However, the reduction of wall thicknesses is limited because it can lead to instability failure (e.g. buckling) [1]. This can be addressed if these areas are strengthened by FRP. Combining metal and FRP structures creates hybrids that outperform singular material solutions in terms of their property profile. By merging the respective material advantages, cost and property increases can be achieved on components that conventionally consist of only one of the two material classes [1, 5].

Hybridization of FRP and metal can be basically divided into two types, post-mold-assembly (PMA) and in-mold-assembly (IMA). A distinction is made as to whether the shaping of the FRP takes place together with the joining process to the metal (IMA) or separately (PMA) [5]. For example, Pöhler et. al. developed a hybrid axle beam. The aluminum upper shell was finished based on various forming and welding operations, while the GMT lower shell was compression molded. Subsequently, both components were reheated to produce an operationally stable joint based on a thermally activatable bonding agent. Despite a significant weight saving of 30 % compared with the steel reference, a considerable (energy) effort is required for production [6].

Based on this, Stallmeister et. al. developed a process in which a bending load optimized beam structure can be produced in one process step. For this purpose, two metal sheets are inserted into the heated mold to enable activation of the adhesion promoter film via the mold wall. Subsequently, GMT material is inserted, shape is formed and the connection between GMT and metal is enabled. In contrast to [6] significantly shorter cycle times and lower energy inputs are realized since no additional energy is required for hybridization [7]. In addition, there are several projects that integrate forming of the metal in the IMA process [8, 9].

Most of joints between FRP and metal are based either on a form fit (micro or macro level), direct adhesion of plastic and metal, or an additional adhesion promoter layer that enables the adhesive behavior between tFRP and metal [10]. Using mechanical joining elements is not advantageous due to potential damage to the fibers and a potential corrosion problem [11]. While micro-form-fit of metal-PP is not practical due to the low polarity of PP, form-fit joining based on undercuts often requires a design adaptation of the reinforcement system [10, 12]. Adhesive bonded connections are possible without design adjustments, guarantee full-surface force application and thus homogeneous stress distribution. However, systems must be used that cure within the usual cycle times for the molding process, so that no further fixing of the joint is necessary [13].

## 2 PROCEDURE / METHOD

To use hybrid compression molding based on an adhesion promoter, knowledge about the effect on the process parameters on joint formation and resulting joint strength is required. In order to study such connections, it is necessary to use a suitable specimen geometry. Due to the fact that it is not practical to use complex component geometries for this purpose, proven abstracted specimen shapes are used. Since bonded joints develop their maximum performance under shear loading, two specimen geometries are used that induce shear stress in the interface. By comparing the different test methods, the joint behavior can be investigated and a geometry can be selected for detailed analysis.

Based on Design of Experiments, the main process parameters for the fabrication of planar hybrid specimens are defined and varied. This is to analyze the effect of the parameters on joint strength and to maximize the strength of the joint by means of a target size optimization. Here, special focus is placed on temperatures acting in the materials and in the mold. In addition to the pure joint strength, the resulting failure behavior of the joint is also considered.

Furthermore, application cases with low and high material flow paths in the forming of the GMT are considered in order to analyze whether strength-minimizing effects occur in the boundary layer of FRP and metal as a result. For the application with a minimum amount of relative motion in the boundary layer, further investigations are carried out to determine the behavior of the hybrid joint under relevant types of loading. This includes a determination of the strength under temperature load, a corrosion change test and a fatigue strength analysis.

## 3 EXPERIMENTAL INVESTIGATIONS

### 3.1 Materials

Two commercially available GMT types with different fiber mass fractions from Mitsubishi Chemical Group are used for the investigations. The chopped fibers of the GMT are randomly orientated. An organic sheet with oriented continuous fibers from company W8SVR GmbH with an orthotropic property profile serves as a reference. All GFRP materials are based on PP. The properties noted in Table 1 are based on the molded condition. The metal used is a 1.5 mm thick aluminum sheet of alloy EN AW-5754 with condition H22 (cf. Table 1). All material properties in Table 1 are based on the respective data sheets of the material suppliers. For bonding, the spray-based adhesion promoter PowderBond$^{PP}$ from Powdertech Surface Science is applied to the aluminum with an initial layer thickness of 300 µm. Before coating, the sheets are first cleaned and chemically pretreated.

| Material | Density (g/cm³) | Fiber content (wt-%) | Young's modulus (GPa) | Tensile strength (MPa) |
|---|---|---|---|---|
| *EN AW-5754 H22* | 2.66 | - | 70 | 235-251 |
| *GMT PP-GF33* | 1.16 | 33 | 4.6 | 70 |
| *GMT PP-GF52* | 1.40 | 52 | 8.6 | 145 |
| *Woven PP-GF70* | 1.65 | 70 | 19.5 | 425 |

Table 1: Material properties of the used aluminum alloy and GFRP.

## 3.2 Manufacturing

A molding tool with a planar die and punch is used to produce the hybrid specimens. The area of the cavity is approx. 5779 mm² (40 mm x 145 mm, r = 5). Both mold halves can be tempered independently via electrical heating elements. A seal against escaping molding material between the punch and die is provided by a fit with a manufacturing tolerance of a few hundredths of a millimeter. The molded specimens can be ejected after the pressing process via a manually operated ejector unit (cf. Figure 1a).

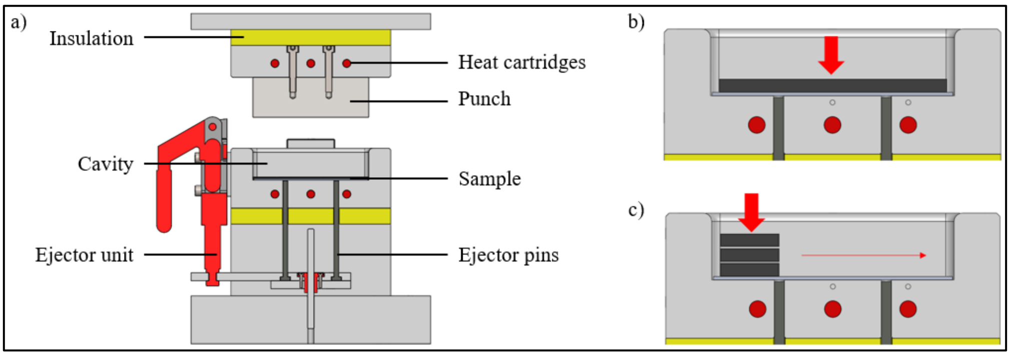


Figure 1: a) Cut view of compression molding tool, b) manufacturing scenario 1, c) manufacturing scenario 2

In preparation for production, the coated aluminum sheets and the GFRP are cut to size on a plate shear. The initial thickness, thickness after molding, width and length as well as the number of layers used are noted in Table 2. The dimensions of the cuttings shown represent a compromise between maximum filling of the cavity and reliable transfer.

| Material | Width and length of cuttings (mm) | Number of layers (-) | Initial thickness (mm) | Molded thickness (mm) |
|---|---|---|---|---|
| *EN AW-5754 H22* | 35 x 140 | 1 | 1.50 | 1.50 |
| *GMT PP-GF33* | 30 x 130 | 1 | 5.40 | 3.90 |
| *GMT PP-GF52* | 30 x 130 | 1 | 4.80 | 3.00 |
| *Woven PP-GF70* | 30 x 130 | 2 | 1.50 | 1.90 |

Table 2: Dimensions of the cuttings for used aluminum alloy and GFRP.

For production, the GFRP is heated for a defined time (GMT: 10 min, organic sheet: 8 min) in a 250 °C convection oven of the company Nabertherm, type TR 240. In accordance with this, the sheet material is heated in the same oven or tempered via the uncoated side using long-wave infrared radiators from company Freek to activate the adhesion promoter. The infrared radiators are power-controlled so that the resulting sheet temperature can be achieved over defined heating times. Corresponding temperature measurements for calibration were carried out in advance. After both components have completed their heating cycle simultaneously, the heated GFRP is placed on the metal sheet while the metal is still in the furnace or on the infrared heating station. This should minimize the temperature loss in the interface and enable an initial bond between the molten adhesion promoter and GFRP.

Subsequently, the stack is transferred to the cavity and hybridized by a servo-motorized screw press of the type 1M-300 from company Synchropress using a previously defined stroke speed, forming pressure and holding time. The forming pressure p is set using the known area of the cavity A and the set pressing force F (cf. Equation 1). The resulting thicknesses of the GFRP components are noted in Table 2. Since the sheet is minimally smaller than the cavity, GMT flows around the sheet at the surrounding edges. The subsequent specimen size is equal to the previously mentioned cavity footprint. After the holding time has passed, the press returns to the starting position and the specimen can be ejected manually.

$$p = F/A \tag{1}$$

Within manufacturing, a distinction can be made between two scenarios. In the first case, forming with a minimal amount of resulting flow of the GFRP is considered (cf. Figure 1b). In the second case, which is only relevant for the GMT, the GMT blank is divided into three equal pieces before heating and stacked on the left side of the cavity. The punch movement causes a relative movement between the GMT and the adhesion promoter (cf. Figure 1c). As a result, the influence of material flow movements in the manufacturing process on the adhesion promoter and the resulting bond strength can be investigated.

### 3.3 Sample preparation and test methods

Since adhesive layers are essentially designed for shear loading, two specimen geometries that induce a high proportion of shear loading in the interface are used and compared to evaluate the bond strength. For this purpose, a lap shear test geometry based on DIN 65148 – hereinafter referred to Single Lap Joint (SLJ) – and a compressive shear test based on patent EP 3 073 244 B1 – hereinafter referred to as Shear-Edge (SE) test – are applied [14]. Both geometries can be cut out of the produced hybrid plates with low heat and distortion using a Cuto wet grinder. For lap shear geometry, additional 2 mm wide grooves are inserted by milling. Production is carried out in stages, so that damage to the base material below is prevented. As with the shear-edge specimens, the resulting joint zone is 25 mm wide and 12.5 mm high, so that a direct comparison between the determined shear stresses can be made in terms of size-dependent flaws or similar (cf. Figure 2).

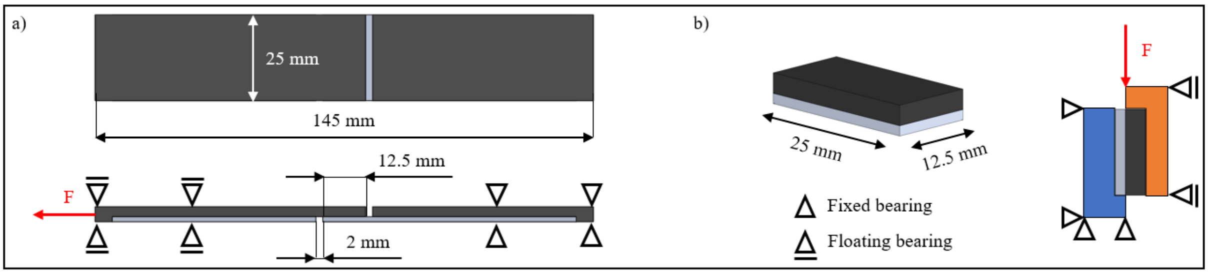


Figure 2: Geometry and test principle of a) Single Lap Joint sample and b) Shear-Edge sample

Depending on the test scenario, tests are performed on a servo-electric (type: Criterion C45.105) and hydraulic (type: 810) universal testing machine from MTS with a constant displacement control of 5 mm/min in tension respectively compression direction. On the hydraulic testing machine, it is possible to carry out cyclic tests and to set defined temperatures. Temperature test is made possible by an insulated test chamber in combination with an air-conditioning unit (type: KSA 320/70 LK - PR 125) supplied by company RS-Simulatoren. Reference tests are performed to ensure that the results are independent of the selected testing machine.

The SLJ experiments are accompanied by an optical displacement measurement based on digital image correlation (DIC) from Carl Zeiss GOM Metrology (type: 4M). A digital microscope of the company Keyence of the type VHX5000 is used to examine the fracture surfaces or boundary layers.

## 4 RESULTS

### 4.1 Suitability and selection of the specimen geometry

For the analysis of the joint, a suitable specimen geometry should be selected, which induces a high proportion of shear stress in the boundary layer. The requirement for an acceptable result is that the joint fails via an adhesion failure of the adhesion promoter to the GFRP or metal, or by a cohesion failure within the adhesion promoter. Fracture or plastic deformation of the metal or GFRP is not acceptable. In the series of tests shown, all specimens were manufactured with the parameters shown in Figure 3. The metal temperature refers to the temperature at the end of the heating cycle, based on heating for 3 min and 20 sec in the 250 °C convection oven. 3 SLJ samples and 5 SE samples were tested per combination. When looking at the results, there is a strong dependence on the sample geometry used. While the results of the SE test are almost constant, the SLJ test shows a strong correlation to the fiber content. Only when using the organic sheet, the joint strengths are at a similar level.

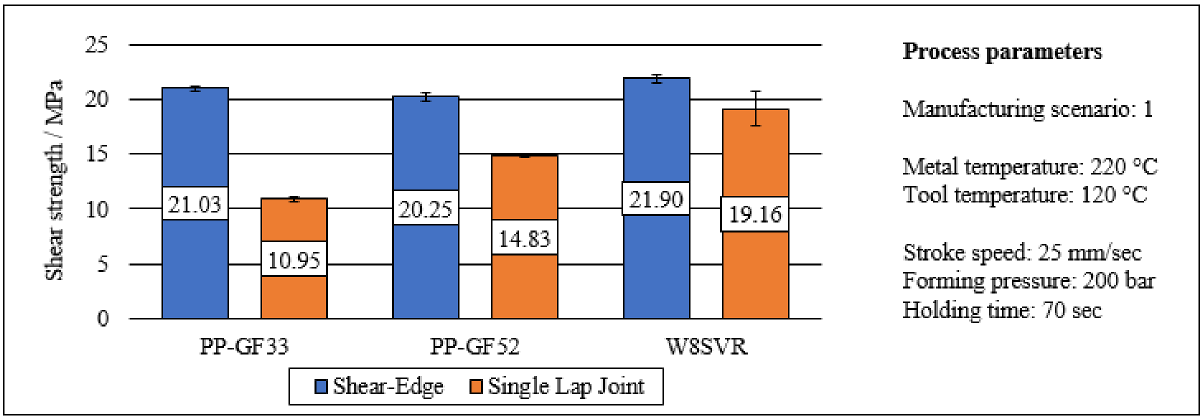


Figure 3: Results of joint testing based on specimen geometry and material combinations.

As already found in some investigations, a bending moment is induced in the SLJ specimen geometry due to the eccentric force application and the resulting force flow [15]. In contrast, the design of the Shear Edge Test fixture prevents specimen tipping, minimizing normal stress on the joint [14]. This is evident when the DIC images of the SLJ specimens just before force decay are considered. While the displacement in the y-direction is largest for the lowest fiber content (PP-GF33), it is minimum for the highest fiber content (W8SVR) (cf. Figure 4a). Due to large deformation, cracks are introduced into the GFRP for both GMT grades, so the results cannot be used (cf. Figure 4b).

Although strengths in the Shear-Edge test are significantly higher, there are differences when looking at the boundary layer after testing. With increased fiber content in GMT (PP-GF52), shear stress is so large that failure of the fiber-matrix bond occurs, leading to failure of the GFRP. Only when a lower fiber content (PP-GF33) or other fiber architecture is used the joint fails mainly via cohesive failure of the adhesion promoter and secondary to adhesion failure to the metal (cf. Figure 4c). For this reason, GMT type PP-GF33 will be used and characterized by the SE method in the following to analyze and optimize the joint formation.

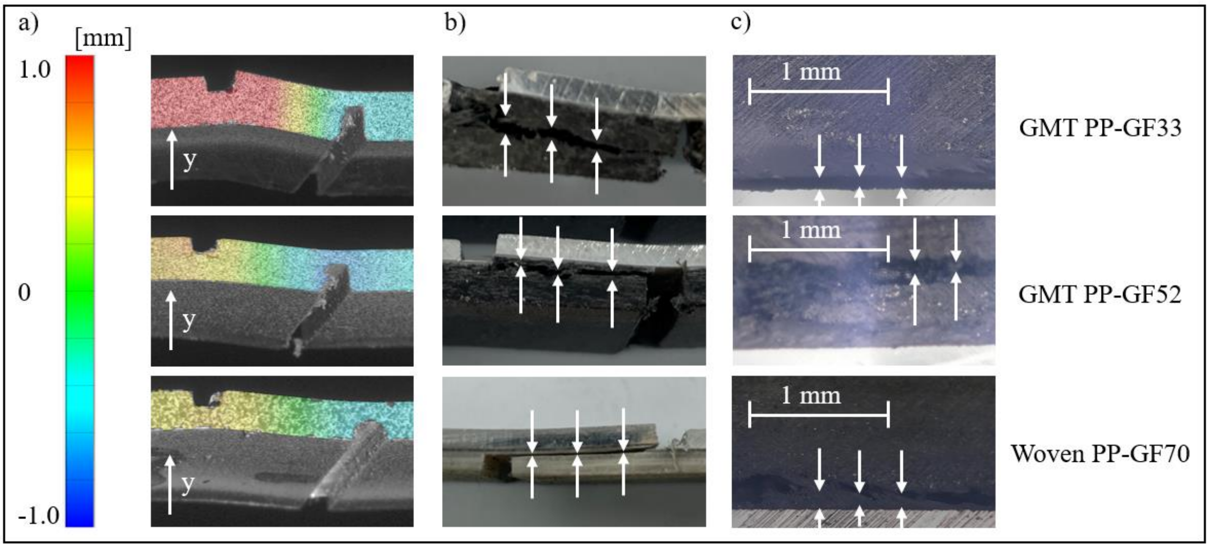


Figure 4: a) DIC measurement of y-displacement of SLJ specimens, b) Resulting failure behavior with marking of the crack, c) Failure of SE specimens in the boundary layer.

### 4.2 Effect of process parameters on joint formation

In order to be able to investigate joint formation of the hybrid connection, various parameters must be taken into account in the manufacturing process. While the coating process by the adhesion promoter manufacturer is considered to be set, several experiences from past work are available in the processing of the GMT [6, 7]. Therefore, the heating of the GMT is carried out for 10 min in a convection oven with the temperature of 250 °C to maximize the mechanical properties of the GFRP. The other parameters investigated and varied in this study are listed below.

- Heating method and heating rate of the metal
- Temperature of the metal sheet (and thus of the adhesion promoter)
- Temperature of the forming tool
- Stroke speed of the punch
- Forming pressure
- Holding time

As mentioned at the beginning of this article, the metal sheet can be heated using a convection oven and a single-sided infrared heating system. Due to the different mechanisms of functioning, significantly higher heating rates are possible via infrared heating. To avoid degradation of the temperature-sensitive adhesion promoter film, only heating via uncoated side is applied. In this way, heat is introduced via the metal and transferred smoothly to the adhesion promoter.

In order to consider the effect of different heating rates, the test point from Figure 3 is carried out with power-controlled infrared heating of 60 % (heating time: 4 min 30 sec) and 100 % (heating time: 1 min 45 sec) for same target temperature of 220 °C. The evaluation results in a minimum deviation of 1 % from averaged joint strength per test series. Based on these findings, infrared heating with 100 % power control will be used for the next series of tests, as this allows the process time to be minimized. Furthermore, this method is less sensitive to operator influences in the course of repeated opening of the furnace door and related temperature fluctuations.

In order to investigate the remaining process parameters from the list, methods of design of experiments are used (DoE). Thus, it is possible to reduce the overall experimental effort and to determine the interaction of factors with each other. First, a screening experimental design is used to investigate the basic influence of factors for two factor levels. Using this method, it is possible to assess with relatively little effort whether the factors have a significant influence on the target value "bonding strength". Due to consideration of two levels, only linear influences of the factors can be identified. If a full factorial design plan was used, five factors (k) would result in a trial size (m) of 32 trial points (cf. Equation 2) [16].

$$m = 2^k \tag{2}$$

By using a fractional factorial screening design plan, the experimental size is halved to 16 experimental points based on logical relationships and mathematical formulas (resolution: V). For more detailed information on statistical design of experiments please refer to [16]. Figure 5 shows the effect of the factors based on the respective factor levels considered. The factor levels have been selected on the basis of common values in the compression molding process. For statistical validation, each test point is produced 3 times and 2 Shear Edge samples are tested in each case. An averaged joint strength was calculated for evaluation.

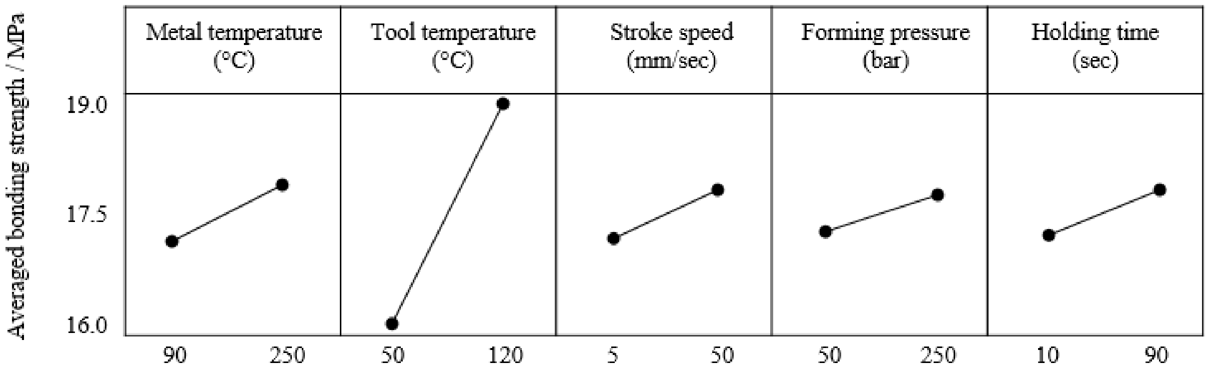


Figure 5: Principle effect chart for bonding strength with corresponding factor levels.

| Process parameter | F-value | p-value |
|---|---|---|
| *Metal temperature (°C)* | 3.01 | 0.11 |
| *Tool temperature (°C)* | 33.11 | 0.00 |
| *Stroke speed (mm/sec)* | 1.32 | 0.28 |
| *Forming pressure (bar)* | 1.43 | 0.26 |
| *Holding time (sec)* | 2.08 | 0.18 |

Table 3: Variance analysis with F- and p-values to determine the influence on joint formation.

Whether a factor has an effect on the target variable can be seen from the gradient in Figure 5 and from the F-value in Table 3. However, the influence cannot be described with certainty via the F-value alone, since a cause-effect relationship must be present. The p-value is used to confirm this effect relationship. The lower the p-value, the higher the probability that the effect did not occur by chance. At a confidence interval of 95%, for $p > 0.05$ there is no evidence of a relationship. For p-values between 0.05 and 0.01, more data are required and only from values $< 0.01$ there is a confirmed influence [16].

On this basis, a reliable influence on the joint strength can only be identified for the tool temperature. Accordingly, the higher the tool temperature, the higher the joint strength. All other factors, including the simple interaction of the factors with each other, have no influence on the target value according to the evaluation. However, it must be taken into account that tool temperature has a direct influence on metal temperature in the forming and joining process. In addition, only linear influences can be identified within the set factor limits, so that quadratic effects cannot be recorded. Therefore, a detailed analysis is carried out for the factors mold temperature and metal temperature via a response surface design plan, so that an optimum can subsequently be defined for these parameters [16]. For the remaining parameters, the common values from the compression molding process are assumed (stroke speed: 25 mm/sec; forming pressure: 150 bar; holding time: 60 sec).

The experimental design with the resolution "V" results in 14 experimental points for the two factors [16]. Again, 3 specimens are prepared per test point and 2 Shear Edge specimens are tested from each. The factor levels examined are shown below.

- Metal temperature [°C]: 50, 87, 175, 243, 300
- Tool temperature [°C]: 50, 62, 90, 118, 130

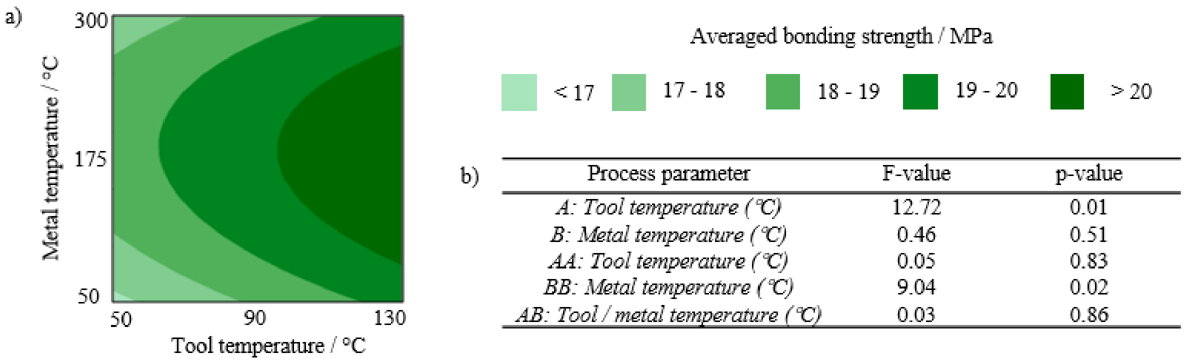


b)

| Process parameter | F-value | p-value |
|---|---|---|
| *A: Tool temperature (°C)* | 12.72 | 0.01 |
| *B: Metal temperature (°C)* | 0.46 | 0.51 |
| *AA: Tool temperature (°C)* | 0.05 | 0.83 |
| *BB: Metal temperature (°C)* | 9.04 | 0.02 |
| *AB: Tool / metal temperature (°C)* | 0.03 | 0.86 |

Figure 6: a) Contour plot for tool and metal temperature factors, b) Corresponding F- and p-values of linear and quadratic factors, as well as the interaction.

The evaluation of several factor levels confirms that linear influence of the tool temperature (A) has a significant influence on the target variable. In addition, the evaluation shows that the metal temperature has a quadratic influence (BB) (cf. Figure 6b). The combination of the two significant process parameters is shown in the contour plot on the left side in Figure 6a). While the increase in strength with increased tool temperature can be described by a positive linear term, the relationship for metal temperature can be represented by a downward-opening parabola. The mold temperature must be limited to 120 °C, since above this temperature, leakage from the cavity occurs due to the low viscosity of the PP. Optimum preheating temperature for the metal is set at 180 °C.

With the selection of process-standard values for the remaining manufacturing parameters, an optimum joint strength of 21.39 MPa with standard deviation (SD) of 0.66 MPa can be achieved. In the evaluation, with few exceptions, a continuous cohesive failure of the joint can be observed.

### 4.3 Influence of operationally relevant loads on the hybrid joint

After the influence of the process parameters on the joint formation has been investigated and the joint strength has been optimized, it is examined how operationally relevant loads affect the joint. This is to ensure suitability for use in industrial applications. For this purpose, the joint is exposed to a corrosion test, a temperature test and a cyclic fatigue test.

A change test according to Volkswagen PV1210 was carried out for corrosion testing. The test includes a specified sequence of climatic and corrosive loads. Per daily cycle, a four-hour salt spray test (DIN EN ISO 9227), a four-hour ventilation with room air and a 16-hour storage at 40 °C and 95 % humidity (DIN EN ISO 6270-2) are performed. Five repetitions are followed by 2 days with normal climate conditions (DIN 50014). After 3, 6 and 12 weeks, 10 Shear Edge specimens are tested in each case. In all tests, no reduction of the bond strength could be observed, so that the bond is very well suited for such loads.

Moreover, the Shear Edge test was performed in an insulated test chamber at - 20 °C and + 80 °C to investigate the influence of such operating temperatures. The results obtained for different test temperatures are shown in Figure 7. It is clear that the joint strengths increase at low temperatures and decrease significantly at higher temperatures. This is basically due to the mechanical behavior of polypropylene, since the adhesion promoter is also PP based [17]. Furthermore, it can be seen that standard deviation of the results (10 SE specimens per temperature) is significantly larger at low test temperatures. This can be attributed to the fact that there is a high variation of fracture patterns at – 20 °C (4 x cohesive failure, 6 x mixed fracture of cohesive failure and adhesion failure to the metal). Obviously, such high test loads are critical for the adhesion bond to the metal. If this type of failure is filtered out, the averaged bond strength increases significantly and the standard deviation decreases. At + 80 °C, a continuous adhesion failure can be observed, which seems to be the reason for the strength decrease.

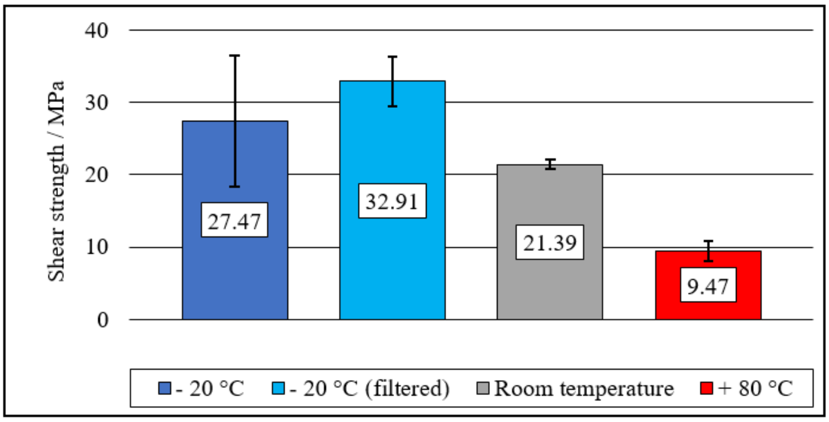


Figure 7: Contour plot for the tool and metal temperature factors together with the corresponding F- and p-values of the linear and quadratic factors, as well as the interaction.

Finally, a force-controlled fatigue strength test of the connection is performed according to DIN EN 9664. This is to ensure that the test also holds reliably under cyclic loads. In addition, fatigue strength tests are well suited to investigate the sensitivity to imperfections in the joint formation. The tests are performed with a constant R-ratio of 0.1 and a frequency of 30 Hz. The respective stress amplitudes can be taken from Figure 8. At least 4 SE specimens are tested per stress amplitude.

The fatigue strength can be reliably described by a compensation line when cohesive failure occurs. In the case of an adhesion failure, the achievable number of cycles is significantly reduced.

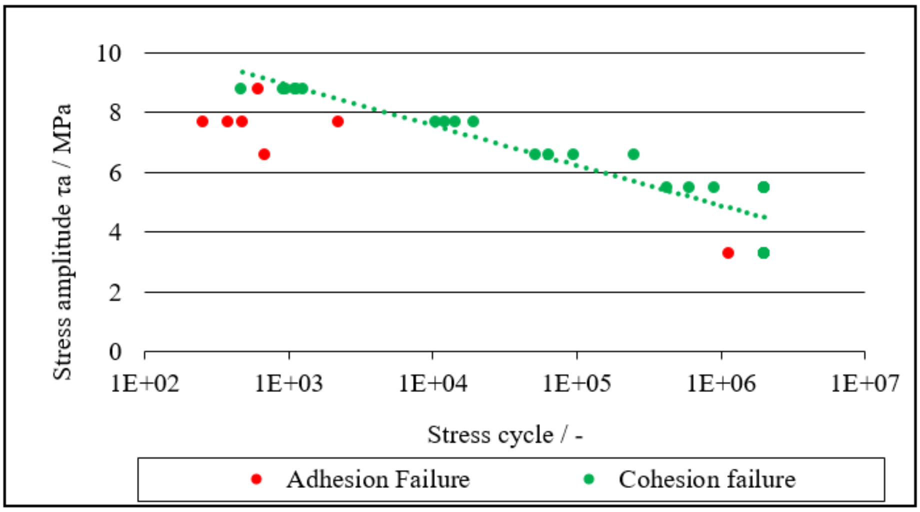


Figure 8: Fatigue strength test according to DIN EN 9664 for a constant R-ratio of 0.1.

### 4.4 Influence of material flow paths in the molding process on joint formation

In the previous study, only the manufacturing scenario from Figure 1b) was considered. In the case of complex hybrid components, however, relative movement between the molten GMT and thermally activated adhesion promoter film can also occur in the course of the molding process (cf. Figure 1c). To investigate this manufacturing condition, the GMT cut (cf. Table 2) is divided into three equal-sized pieces, heated, stacked, inserted at the edge of the cavity and pressed. The previously defined manufacturing parameters are used. However, the stroke speed is varied (5, 25 and 50 mm/sec) to induce different shear rates in the flow process. Subsequently, 4 Shear Edge specimens are cut out, with position 1 being at the position of the material insert (low flow rate) and position 4 being at the other end of the cavity (highest flow distance). Three samples were produced for each stroke speed. The results of the test are shown in Figure 9.

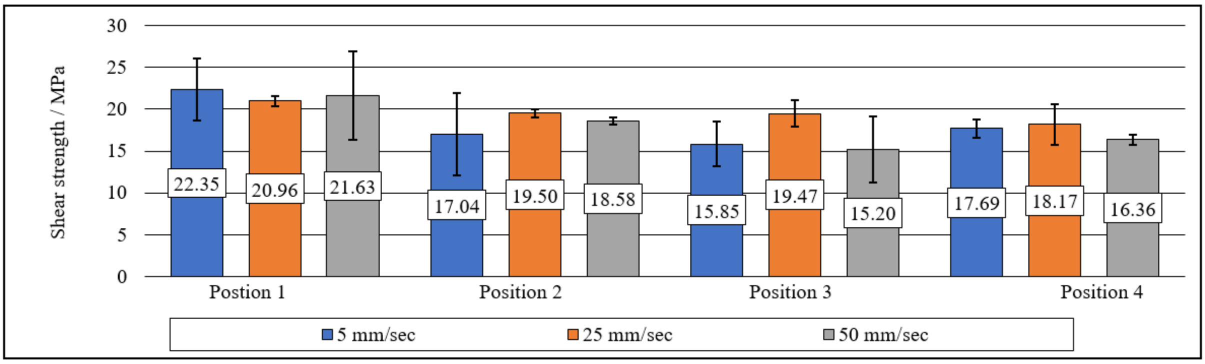


Figure 9: Bond strength as a function of the GMT flow content and the shear rate induced by the stroke velocity.

On the left side of the cavity where the stacked GMT plies are pressed, the strength is comparable to the main tests due to the low material flow rate. As the material flow amount increases, the strength reduces down to 15.20 MPa, while at the right end of the cavity the strength increases again by up to 10 %. The greatest reduction in strength occurs at very low (5 mm/sec) and very high (50 mm/sec) stroke speeds.

Basically, three causes for influencing the resulting bond strength are imaginable. The flowing movement of the GMT can lead to an alignment and depletion or accumulation of the fibers [3]. This assumption could be excluded by making CT scans of the hybrid specimens and density measurements of the GMT. Both analysis methods showed a homogeneous distribution of the fibers.

The second assumption is based on the different transfer method and resulting temperature losses of the adhesion promoter layer. While in the production scenario from Figure 1b) the adhesion promoter is covered by the heated GMT directly after the end of the heating cycle, in the scenario considered here only one third of the surface is covered by the GMT. As a result, the heat cannot be conserved in the boundary layer and temperature losses occur. Additionally, no initial bonding between the GMT and adhesion promoter can be enabled in these areas. Appropriate studies have yet to be conducted on this theory, so no statement can be made at this time.

Most likely, there is relative movement between the heated GMT and adhesion promoter in the pressing process. The determined strengths suggest that the flow front of the GMT displaces the adhesion promoter in flow direction, resulting in an accumulation at the end of the cavity. A corresponding evaluation of the boundary layer thickness in the micrograph and an optical evaluation of the fracture patterns support this assumption. In further studies, a more detailed evaluation based on optical evaluation methods (e.g. gray value analysis) is planned. In addition, on the basis of an extended test plan, it is to be investigated whether an adjustment of the previously defined process parameters can homogenize the joint strength. Reducing the temperatures in the mold or in the metal so that the adhesion promoter layer is more resistant to the flow front of the GMT is conceivable.

## 4 SUMMARY / CONCLUSIONS

Within the presented study, the joint formation of a hybrid GMT-metal joint based on compression molding process was investigated. In the context of requirements for a series production process, the forming of the GMT and the joint formation to the metal are carried out in one process step (in-mold assembly). In order to determine the sensitivity of the joint formation to the process boundary conditions, the relevant process parameters were defined and systematically investigated on the basis of a statistical experimental design. The analysis showed that above all the temperature control - in terms of mold and metal temperature - has a significant influence on the resulting joint strength. Via target size optimization, both parameters were adjusted so that joint strengths of 21.39 MPa with a low standard deviation of 0.66 MPa can be reliably achieved. Compared to similar work for the material combination GMT and aluminum, increases in bond strength of 41 % [7] to 67 % [6] are possible via the selected process control for the Powderbond adhesion promoter system.

An investigation was carried out subsequently for relevant loading cases for the selected process parameter combination. While a corrosion test according to PV1210 did not result in a reduction of the joint strength even after 12 weeks, a sensitive reduction of the strength at elevated service temperatures was noticeable. For a test temperature of + 80 °C, there was a strength reduction of 56 % compared with the test at room temperature. This reduction is associated with an adhesion failure of the adhesion promoter to the aluminum. In further studies, studies on surface modification of the aluminum will be carried out in consultation with the manufacturer of the adhesion promoter system in order to optimize the adhesion properties at high operating temperatures. Since occasional adhesion failures also resulted in scatter in the fatigue test performed, this adjustment is also relevant to the performance of the joint at room temperature.

Finally, it was examined how the relative movements between molding compound and adhesion promoter induced by the molding process influence the bond. By adjusting the insertion strategy of the heated GMT, the bond strength could be evaluated as a function of the position in the cavity. Basically, it was observed that the bond strength is degraded with increased material flow rate. At a stroke speed of 50 mm/sec, this reduction is 29% in the worst case. Similar effects are observed for stroke speeds of 5 mm/sec and 25 mm/sec, but it has not yet been possible to understand why these effects are strongest at very low (5 mm/sec) and very high (50 mm/sec) stroke speeds and most moderate at a medium speed of 25 mm/sec. Further studies will determine the physical basis of these effects. In addition, it will be investigated whether an adjustment of the process parameters or the surface pretreatment of the metal makes it possible to homogenize the joint strength in such process scenarios.

In addition, the joint formation in component-like structures will be analyzed in the future so that it can be verified whether the results can be transferred on the basis of the presented specimens. The hybrid beam structure from [7] is particularly promising for this purpose, since this structure induces a shear stress in the boundary layer in the bending load case. It is interesting to see how the load-bearing behavior is influenced when the bending test is performed at elevated service temperatures.

## ACKNOWLEDGEMENTS

Many thanks go to James Grant and Dr. Nicholas Welton of Powdertech Surface Science for coating the aluminum sheets and discussing the results. Further thanks go to all former and current colleagues as well as students at the Chair for Automotive Lightweight Design who supported this study.

## REFERENCES

[1] B. Klein, T. Gänsicke, *Leichtbau-Konstruktion. Dimensionierung, Strukturen, Werkstoffe und Gestaltung*, Vol. 11, Springer Vieweg, Wiesbaden, 2018 (doi: 10.1007/978-3-658-26846-6).

[2] AVK – Industrievereinigung Verstärkte Kunststoffe e. V., *Handbuch Faserverbundkunststoffe/ Composites*, Vol. 4, Springer Vieweg, Wiesbaden, 2014 (doi: 10.1007/978-3-658-02755-1).

[3] A. Rubio, P. Eguizabal, M.A. Mendizabal and J.F. Liceaga, Influence of the processing parameters on glass mat reinforced thermoplastic (GMT) stamping, *Composites Manufacturing*, **3**, 1992, pp. 47- 52 (doi: 10.1016/0956-7143(92)90183-U).

[4] J.L. Thomason, The influence of fibre length and concentration on the properties of glass fibre reinforced polypropylene: 5. Injection moulded long and short fibre PP, Composites Part A, 33, 2002, pp. 1641-1652 (doi: 10.1016/S1359-835X(02)00179-3).

[5] D. Drummer et al., *Handbuch Kunststoff-Metall-Hybridtechnik*, Lehrstuhl für Kunststofftechnik, Erlangen, 2015.

[6] S. Pöhler, *Konzeptionierung und Auslegung eines Vorderachsträgers in hybrider Leichtbauweise im C-Segment*, Vol. 1, Shaker-Verlag, Düren, 2021.

[7] T. Stallmeister, *Verfahrensentwicklung zur einstufigen Herstellung von biegebelastbaren Hybridstrukturen im Fließpressprozess*, Vol. 1, Shaker-Verlag, Düren, 2023.

[8] D. Heidrich, T. Klosa, X. Fang, Universität Siegen: MultiForm. *Abschlussbericht zum BMBF-Forschungsprojekt*, Reihe AUTOMOBILTECHNIK (2019), Vol. 3, Siegen 2019.

[9] Forel Forschungs- und Technologiezentrum für Ressourcen effiziente Leichtbaustrukturen der Elektromobilität: *Q-Pro Qualitätsgesicherte Prozessketten-verknüpfung zur Herstellung höchstbelastbarer intrinsischer Metall-FKV-Verbunde in 3D-Hybrid-Bauweise*, Dresden, 2013.

[10] M. Grujicic et. al., An overview of the polymer-to-metal direct-adhesion hybrid technologies for load-bearing. *Journal of Materials Processing Technology*, **197**, 2008, pp. 363-373 (doi: 10.1016/j.jmatprotec.2007.06.058).

[11] U. Reisgen et. al., Innovative joining technology for the production of hybrid components from FRP and metals. *Journal of Materials Processing Technology*, **282**, 2020 (doi: 10.1016/j.jmatprotec.2020.116674).

[12] X. Li, F. Liu, N. Gong, P. Huang, C. Yang, Enhancing the joining strength of injection-molded polymer-metal hybrids by rapid heating and cooling, *Journal of Materials Processing Technology*, **249**, 2017, pp. 386-393 (doi: 10.1016/j.jmatprotec.2017.06.034).

[13] L. Li, L. Sun, Z. Dai, Z. Xiong, B. Huang, Y. Zhang, Experimental investigation on mechanical properties and failure mechanisms of polymer composite-metal hybrid materials processed by direct injection-molding adhesion method, *Journal of Materials Processing Technology*, **263**, 2019 (doi: 10.1016/j.jmatprotec.2018.08.039).

[14] K. A. Weidenmann, *Vorrichtung und ein Verfahren zur Bestimmung der Scherfestigkeit und des Schermoduls von Verbundwerkstoffen*, Patent EP3073244A1, Germany, 2016.

[15] R. Garcia, T.A. Weisshaar, R.R. McWithey, An Experimental and Analytical Investigation of the Rail Shear-test Method as Applied to Composite Materials, *Experimental Mechanics*, **20**, pp. 273-279, 1980.

[16] W. Kleppmann, *Versuchsplanung: Produkte und Prozesse optimieren*, Vol. 10, Hanser, Munich, 2020.

[17] B. Alcock et. al., The effect of temperature and strain rate on the mechanical propertiesof highly oriented polypropylene tapes and all-polypropylene composites, *Composites Science and Technology*, **67**. 2007, pp. 2061-2070 (doi: 10.1016/j.compscitech.2006.11.012).